# Surface Studies of Polystyrene–Poly(methyl Methacrylate) Diblock Copolymers Precipitated by Different Precipitants

JEONGIN SOHN and TAIKYUE REE, *Department of Chemistry, Korea Advanced Institute of Science and Technology, P.O. Box 150 Chongyangni, Seoul, Korea*

## Synopsis

Diblock copolymers of polystyrene (PS) and poly(methyl methacrylate) (PMMA) with varying compositions in the mole fractions of PS were prepared, and were obtained in particle state by different methods of precipitation. The morphology of the precipitates was studied by electron spectroscopy for chemical analysis (ESCA), scanning electron microscopy (SEM), differential scanning calorimetry (DSC), and viscometry. From these studies it was found that the precipitates of diblock copolymers have core-micelle structures, the components of the core and the surrounding micelle being different by precipitation histories.

## INTRODUCTION

Heterocomponent nature of block copolymers gives many interesting problems of polymer science. Surface properties of block copolymers are one of the related problems of this nature.[1,2] Surface exess phenomena are well-known properties of heterocomponent polymers when casted by various solvents in film states.[3-6] Various interesting properties of block copolymers are found in the recent books.[7-9]

In this article, the surface compositions of PS–PMMA diblock copolymers in powder state which are precipitated in different nonsolvents are the main concern. To study powder-state surfaces, electron spectroscopy for chemical analysis (ESCA) was used. ESCA derives 90% of peak intensities from the surface layers of topmost 27 Å in thickness.[10,11] PS–PMMA diblock copolymers with various compositions were used as samples. Intrinsic viscosity measurements, electron microscopy, and differential scanning calorimetry (DSC) were used for supporting the ESCA results.

## EXPERIMENTAL

### Sample Block Copolymers

PS–PMMA diblock copolymers were prepared by the typical anionic living polymerization technique[12,13] using $n$-BuLi as an initiator, tetrahydrofuran (THF) as a polymerization solvent, and $n$-BuOH as a terminator.

The syndiotactic nature of PMMA segments was observed by NMR as Bovey and Tiers reported.[14] Syndiotactic $\alpha$-methyl peaks at $\delta = 0.91$ was

strongest, heterotactic peaks at $\delta = 1.05$ was moderate, and isotactic at $\delta = 1.22$ was almost always indetectible. Mole fractions of PS were also measured by NMR spectroscopy. Weight averaged molecular weights of the block copolymers were measured by a light scattering method by using THF as a solvent. Polydispersities of the block copolymers were determined by a gel permeation chromatography (GPC) using THF as an eluent. We chose five samples which have different mole fractions of PS and moderate molecular weights as shown in Table I.

## Precipitation

For each block copolymer, a THF solution of 0.1 wt % was prepared. Thirty milliliters of the solution was dropped slowly into 300 mL of methanol stirring vigorously. The precipitate was in powder form. By a similar method the precipitate in kerosene was obtained. In this case, however, the precipitate of PS-rich block copolymers obtained at 25°C was rather in sticky state. But, at about −20°C, we could easily obtain the precipitate in fine particle state. All the precipitates obtained by the above procedures were filtered and dried in a vacuum oven ($10^{-4}$ torr) for over 72 h at room temperature. (Note: The characteristic properties of the sample in Table I are not affected by the precipitation procedures.)

## ESCA Measurements

ESCA spectra were obtained on an electron spectra (Perkin-Elmer PHI model 2100) using an Al $K_\alpha$ radiation (1486.7 eV). Sample powders were prepared to pellets after grinding and pressing. Experimental conditions were fixed at 9 kV X-ray voltage and 28 mA of emission current. The $1s$ oxygen peaks were at $534.7 \pm 0.5$ eV and the $1s$ carbon peaks were at $288.0 \pm 0.5$ eV on the spectra. The relative surface population of oxygen to carbon ($I_0/I_C$) was obtained from the peak area of each spectrum: This ratio is a measure of the surface compositions of PMMA and PS on the surface of a sample block copolymer. In Table II, the ratios of $I_0/I_C$ for 10 samples of block copolymers and PMMA and PS homopolymers are tabulated. The ratios of $I_0/I_C$ for pure PMMA and PS were 0.84 and 0.05, respectively (see Table II). Here one notes that only a small amount of oxygen adsorbed on the PS surfaces was detected. Experimental reproducability of the ratios was better than 5%.

TABLE I
Characteristics of Sample Block Copolymers

| Samples | B1 | B2 | B3 | B4 | B5 |
|---|---|---|---|---|---|
| Mole fractions of PS,[a] $x$ | 0.86 | 0.78 | 0.48 | 0.21 | 0.13 |
| Molecular weight[b] $\times 10^{-4}$ | 25.0 | 4.8 | 4.0 | 13.0 | 8.7 |
| Polydispersity[c] | 1.23 | 1.12 | 1.12 | 1.13 | 1.06 |

[a] Measured by a NMR spectroscopy.
[b] Measured by a light scattering method.
[c] Measured by a GPC.

TABLE II
Intensity Ratios of Oxygen to Carbon on the Surfaces of Sample Block Copolymers which Were Measured by the ESCA Spectrograms

| Samples | B1 | B2 | B3 | B4 | B5 | PS | PMMA |
|---|---|---|---|---|---|---|---|
| $I_0/I_C$ MeOH[a] | 0.25 | 0.32 | 0.83 | 0.85 | 0.89 | 0.05 | 0.84 |
| $I_0/I_C$ kerosene[a] | 0.08 | 0.04 | 0.38 | 0.65 | 0.57 | | |

[a] Indicates the precipitant by which the samples of the diblock copolymers were precipitated.

## Intrinsic Viscosity Measurements

Intrinsic viscosities were measured for four cases of different solvent systems (Table III) using a Ubbelohde type viscometer. The temperature was $25 \pm 0.1°C$.

Case 1 is a solvent system of THF, cases 2 and 3 are the THF/methanol mixture–solvent systems of volume ratio 10:4 and 10:7, respectively. Case 4 is the THF/kerosene mixture–solvent system of volume ratio 10:4. In cases 1 and 2, all the sample block copolymers, PS, and PMMA homopolymers were soluble. In case 3, PS and PS-rich block copolymers were insoluble (opaque). In case 4, in contrast to case 3, PMMA and the PMMA-rich block copolymer B4 were insoluble.

## Electron Microscopy

Scanning electron microscopy (SEM) studies were carried out by using ETEC Autoscan Model 149-10. The five pairs of powder-state samples (in Table II) prepared as described in the Precipitation paragraph were used. The aggregation states and particle sizes were different when a given block copolymer solution was treated in different routes of precipitation as shown in Figure 1. The detailed explanation of Figure 1 will be given later.

TABLE III
Intrinsic Viscosities of Block Copolymers in Various Solvent Systems[a]

| Samples | B1 | B2 | B3 | B4 | B5 |
|---|---|---|---|---|---|
| Case 1 (THF) | 0.847 | 0.256 | 0.245 | 0.588 | 0.402 |
| Case 2 (THF:MeOH=10:4) | 0.620 | 0.202 | 0.217 | 0.493 | 0.326 |
| Case 3 (THF:MeOH=10:7) | Opaque | Opaque | 0.204 | 0.388 | 0.314 |
| Case 4 (THF:Kero=10:4) | 0.686 | 0.177 | 0.174 | Opaque | 0.201 |

[a] Units in dL/g.

a   (B1)  ⟷ 1μ              b   (B2)  ⟷ 1μ

c   (B3)  ⟵ 1μ             d   (B4)  ⟶ 1μ
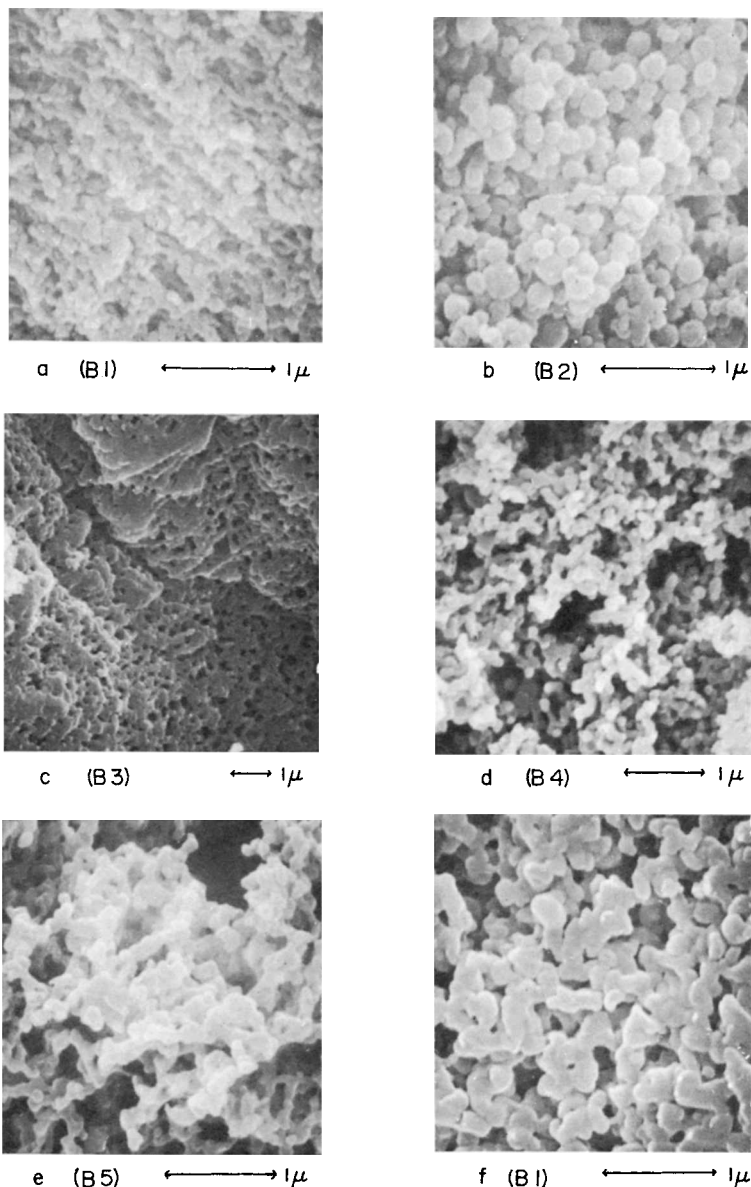
e   (B5)  ⟷ 1μ             f   (B1)  ⟷ 1μ

Fig. 1.   Scanning electron micrograms (SEM) of diblock PS–PMMA copolymers: (a–e) precipitates obtained in methanol; (f–j) precipitates in kerosene. Samples B1–B5 are characterized in Table I.

## DSC Measurements

Differential scanning calorimetry (DSC) studies were conducted on the five pairs of sample block copolymers in fine powder states. A high-performance DuPont Model 910 DSC machine was used. Scanning rate of temperature was 10°C/min in nitrogen atmosphere and over the temperature range of 40–140°C. Almost all the thermograms of $d(\Delta H/dt$ vs. temperature were highly reproducible from the third thermogram for each sample.

g   (B 2)                    ↤ 1μ



h   (B 3)                    ← 1μ



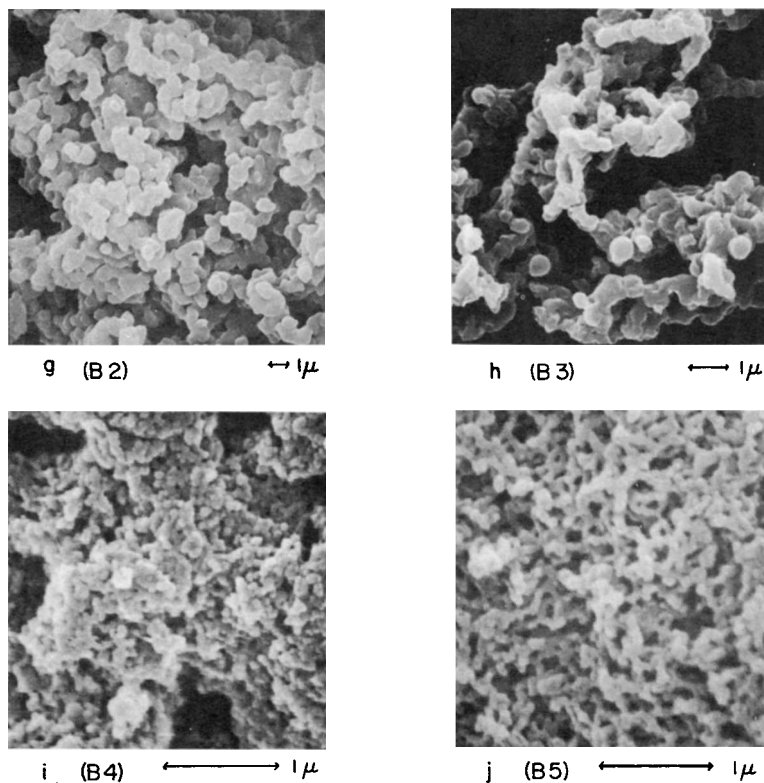i   (B 4)      ←——————→ 1μ



j   (B 5)      ←——————→ 1μ

Fig. 1.   *(Continued from previous page.)*

## RESULTS

Five sample block copolymers were characterized as shown in Table I. Mole fractions of PS component, molecular weights, and polydispersities were measured by using the method described under Experimental.

In Table II, the ESCA data of $I_0/I_C$ are tabulated. The ratios of oxygen to carbon peaks are always larger when the precipitant is methanol than when it is kerosene. Particularly, one may note that the PMMA-rich samples, B3, B4, and B5 have the ratio of $I_0/I_C$ similar to that of the pure PMMA, 0.84 (Table II). One may also note that surfaces of PS-rich block copolymers B1 and B2 show only small amounts of oxygen when kerosene is a precipitant. Such surface excess phenomena give some hints for the core-micelle structure of precipitates (see under Discussion).

Figure 1 shows the SEM micrographs of the particles with different precipitation histories. The PS-rich samples of B1 and B2 precipitated in methanol show good particle shape [see Figs. 1(a) and 1(b)], but the sample B3 and the PMMA-rich samples of B4 and B5 obtained all in methanol [see Figs. 1(c), 1(d), and 1(e)] show rather aggregate shape. The contrary is true for precipitates obtained in kerosene, i.e., the samples of B4 and B5 [Figs. 1(i) and 1(j)] have good particle shape while the samples B1, B2, and B3

show aggregation state [Figs. 1(f), 1(g), and 1(h)]. From Figure 1, one notes that the SEM experiments show different nonsolvent effects of methanol and kerosene, which will be discussed later in this article.

Intrinsic viscosity results are shown in Table III. Intrinsic viscosity, which is a function of the dimension of a sample polymer in solution, decreases by feeding nonsolvents to the solution. (Compare the second row data with those in the third row.) The decrease in $[\eta]$ is selective to the nonsolvents. The $[\eta]$ of B2 is larger than that of B3 in THF (see case 1 in Table III), but $[\eta]$ of B2 is smaller than that of B3 when small amount of methanol is added to THF (case 2). When more methanol is added (case 3), the PS-rich B1 and B2 go through the cloud point and show precipitation (opaque). In case 4, the PMMA-rich block copolymers B4 and B5 are more subject to the precipitation because of the selectivity of kerosene to PMMA. For B4 in case 4, the molecular weight of PMMA in the block copolymer is 10.27 $\times\ 10^4\ (=\ 13.0\ \times\ 10^4\ \times\ 0.79)$ whereas for B5 it is $7.6\ \times\ 10^4\ (=\ 8.7\ \times\ 10^4\ \times\ 0.87)$. Thus B4 precipitates while B5, B1, B2, and B3 all do not.

The DSC thermograms of 1:1 block copolymer, B3, show interesting phenomena as shown in Figures 2(a) and 2(b), which are for the B3 samples precipitated in methanol and in kerosene, respectively. Two distinct glass transition temperatures $(T_g)$ were detected at ca. 80 and 100°C on each thermogram, which was reproducible over several scannings. The $T_g$ of syndiotactic and heterotactic PMMA (100°C)[15] appeared more strongly in the methanol treated sample [Fig. 2(a)] than that in the kerosene treated sample [Fig. 2(b)], whereas the reverse is exactly true for the $T_g$ of PS (80°C).

## DISCUSSION

We note from Table III the following facts: When the PS–PMMA diblock copolymers in THF solution (case 1) were deposited by adding enough methanol (case 3), the PS-rich copolymers B1 and B2 precipitate first (see Table III), but when the THF solution was treated by kenosene, the PMMA-rich copolymer B4 deposited preferentially (case 4). (Note: For the reason of
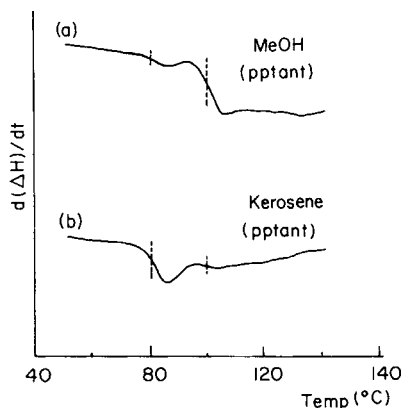


Fig. 2. DSC thermograms diblock copolymer B3 ($x$ = 0.48). Two glass transitions appear at 80°C (for PS) and 100°C (for PMMA): (a) copolymer sample precipitated in MeOH, the glass transition of PMMA appears stronger than that of PS; (b) sample precipitated in kerosene, the glass transition of PS appears stronger than that of PMMA.

nondeposition of B5, mention has already been made under Results.) These experimental facts are rationalized by the idea of the selectivety of precipitants, i.e., the selectivity of methanol for precipitating PS is larger than for precipitating PMMA, whereas the selectivity of kerosene for PMMA is larger than for PS. Thus, for PS-rich copolymers B1 and B2 in case 3 (Table III), the PS segments of the copolymers intramolecularly and intermolecularly aggregate first making a nucleus; then PMMA segments deposit surrounding the nucleus making a particle. In case 4 (Table III) the opposite process occurs, i.e., in the PMMA-rich copolymer B4, the PMMA segments aggregate first by the selectivity of kerosene making a core, then the PS segments deposit around it. Thus the so-called core-micelle structure is established which is different in composition by the history of precipitation.

According to the ESCA experiment (Table II), the particles, which were precipitated by methanol from the THF solution of diblock copolymers, showed larger ratio of $I_0/I_C$ than the case when kerosene was used as a precipitant. That is the surface concentration of PMMA of the former case (precipitant: methanol) is larger than that of the latter case (precipitant: kerosene). This fact is explained by the formation of core-micelle structure. As mentioned above, when methanol was used as a precipitant, the core of a particle of precipitates is composed of PS segments which is surrounded by PMMA segments while the reverse is true when kerosene is used as a precipitant. Thus the ESCA data in Table II are eloquently explained, i.e., the second row data are always larger than the third row data, because the former are due to the PMMA segments of the out-sheath of a particle whereas the latter are responses from the PS segments surrounding the PMMA core.

From Figures 1(a) and 1(b), which are the SEM micrographs for the precipitates of PS-rich B1 and B2 block copolymers obtained by treating the THF solution with the precipitant methanol, one notes that the particle shape of the precipitates is very good whereas the precipitates of PMMA-rich B3, B4, and B5 copolymers shows rather aggregated shape [see Figs. 1(c), 1(d), and 1(e)]. On the contrary, it was found that when the precipitant kerosene was used, the precipitates of PMMA-rich copolymers B4 and B5 show a good shape of particles [see Figs. 1(i) and 1(j)] whereas the PS-rich copolymers show an aggregated shape [see Figs. 1(f), 1(g), and 1(h)]. These experimental facts are also explained by the selectivity of precipitants, i.e., the selectivity of methanol for PS is very large than that for PMMA in methanol; thus the PS-rich B1 and B2 copolymers precipitate in a particle shape in methanol [Figs. 1(a) and 1(b)] while the PMMA-rich B4 and B5 copolymers deposit in an aggregate form [Figs. 1(c), 1(d), and 1(e)]. The reverse facts found in Figures 1(f)–1(j) are similarly explained by the fact that the selectivity of kerosene for PMMA is larger than that of PS.

Next we explain the DSC results in Figures 2(a) and 2(b). Both figures for the sample B3 (the mole fraction of PS $\simeq$ 0.5), which was precipitated in different ways. The B3 block copolymer for Figure 2(a) was precipitated from its THF solution by methanol. In this case, as already mentioned, the PS segments of the block copolymer coagulate first making core; then the outside of the core is surrounded by the PMMA segments making a particle. Thus the thermogram appears like Figure 2(a), i.e., the glass transition

occurring in the PMMA phase of the out-sheath of the particle responses strongly whereas the glass transition in the PS phase in the core responses weakly because of the poor thermal conduction. In Figure 2(b), the B3 sample copolymer was precipitated in kerosene. As mentioned previously, the core of the precipitate is composed of PMMA, the outside of which is surrounded by PS segments. Thus the thermogram [Fig. 2(b)] appears in the opposite way from Figure 2(a), i.e., the glass transition in the PS phase appears strongly while that in the PMMA phase in core weakly.

For other samples B2 and B4, similar phenomena as shown in Figures 2(a) and 2(b) were observed, although not as clear as for sample B3. The results are not shown here.

Returning to Table II, we note that the $I_0/I_C$ ratios of B3, B4, and B5 samples deposited in methanol are equal to that of pure PMMA (0.84). We have pointed out that in the SEM micrographs Figures 1(c), 1(d), and 1(e), the B3, B4, and B5 copolymers make aggregate precipitates. In this case, as mentioned previously, the core of each particle is composed of PS, outside of which are surrounded by PMMA. Thus particles having PMMA in the out-sheath stick together through the attraction between the particles. One may easily understand that the copolymers B3, B4, and B5 in Figures 1(c), 1(d), and 1(e) all have similar surface composition as pure PMMA, i.e., similar $I_0/I_C$.

An analogous fact was found as explained below. In Table II, the block copolymers B1 and B2 deposited in kerosene have the ratios of $I_0/I_C \simeq 0.06$, which is about equal to that of pure PS (0.05). According to the SEM micrographs, Figures 1(f) and 1(g), the particles stick together making an aggregation state. In this case, the core of each particle is composed of PMMA outside of which are surrounded by PS. Because of this reason, the B1 and B2 samples in Table II showed an $I_0/I_C$, which is about equal to that of PS (0.05).

From the above-mentioned facts it may be concluded that the core-micelle structure model is correct.

## References

1. Huynh-Ba-Gia, R. Jérôme, and Ph. Teyssié, *J. Polym. Sci., Polym. Phys. Ed.*, **18**, 2391 (1980).

2. T. Okano, M. Katayama, and I. Shinohara, *J. Appl. Polym. Sci.*, **22**, 369 (1978).

3. P. Bajaj and S. K. Varshney, *Polymer*, **21**, 201 (1980).

4. R. E. Cohen and F. S. Bates, *J. Polym. Sci., Polym. Phys. Ed.*, **18**, 2143 (1980).

5. H. R. Thomas and J. J. O'Malley, *Macromolecules*, **12**, 323 (1979).

6. J. J. O'Malley, H. R. Thomas, and G. M. Lee, *Macromolecules*, **12**, 996 (1979).

7. D. C. Allport and W. H. Janes, *Block Copolymers*, Wiley, New York, 1973.

8. A. Norshay and J. E. McGrath, *Block Copolymers*, Academic, New York, 1977.

9. D. J. Meier, *Block Copolymers*, MMI Press Symposium Series Vol. 3, Hardwood Academic Publishers, New York, 1983.

10. D. T. Clark and H. R. Thomas, *J. Polym. Sci., Polym. Phys. Ed.*, **16**, 791 (1978).

11. D. T. Clark, J. Peeling, and J. M. O'Malley, *J. Polym. Sci., Polym. Chem. Ed.*, **14**, 543 (1976).

12. M. Bear, *J. Polym. Sci., Part A*, **2**, 417 (1964).

13. T. Tanaka, T. Kodaka, and H. Inagaki, *Macromolecules*, **3**, 311 (1974).

14. F. Bovey and G. V. D. Tiers, *J. Polym. Sci.*, **44**, 173 (1960).

15. S. Bywater and P. M. Toporowski, *Polymer*, **13**, 94 (1972).